Neuron, Vol. 38, 555–565, May 22, 2003, Copyright ©2003 by Cell Press

Cdk5 Is a Key Factor in Tau Aggregation and Tangle Formation In Vivo

Wendy Noble,[1] Vicki Olm,[1] Kazuyuki Takata,[1] Evelyn Casey,[1] Mary O,[1] Jordana Meyerson,[1] Kate Gaynor,[1] John LaFrancois,[1] Lili Wang,[1] Takayuki Kondo,[1] Peter Davies,[2] Mark Burns,[1] Veeranna,[1] Ralph Nixon,[1] Dennis Dickson,[3] Yasuji Matsuoka,[1] Michael Ahlijanian,[4] Lit-Fui Lau,[4] and Karen Duff[1,*]

[1]Center for Dementia Research
Nathan S. Kline Institute
New York University
140 Old Orangeburg Road
Orangeburg, New York 10962

[2]Department of Pathology
Albert Einstein College of Medicine
1300 Morris Park Avenue
Bronx, New York 10461

[3]Mayo Clinic
5400 San Pablo Road
Jacksonville, Florida 32224

[4]CNS Discovery
Pfizer Global Research and Development
Eastern Point Road
Groton, Connecticut 06340

Summary

Tau aggregation is a common feature of neurodegenerative diseases such as Alzheimer's disease, and hyperphosphorylation of tau has been implicated as a fundamental pathogenic mechanism in this process. To examine the impact of cdk5 in tau aggregation and tangle formation, we crossed transgenic mice overexpressing the cdk5 activator p25, with transgenic mice overexpressing mutant (P301L) human tau. Tau was hyperphosphorylated at several sites in the double transgenics, and there was a highly significant accumulation of aggregated tau in brainstem and cortex. This was accompanied by increased numbers of silver-stained neurofibrillary tangles (NFTs). Insoluble tau was also associated with active GSK. Thus, cdk5 can initiate a major impact on tau pathology progression that probably involves several kinases. Kinase inhibitors may thus be beneficial therapeutically.

Introduction

Neurofibrillary tangles (NFTs) are a common feature of many neurodegenerative diseases, including Alzheimer's disease (AD). Human NFTs are composed primarily of aggregated tau in paired helical filaments (PHF) which are hyperphosphorylated at several sites (Grundke-Iqbal et al., 1986; Friedhoff et al., 2000). Hyperphosphorylation of tau has been suggested to be a pathogenic process that may impact the initiation, or progression of tauopathy. Several kinases, including the proline-directed, cyclin-dependent kinase-5 (cdk5), have been implicated as candidates in pathogenic tau phosphorylation. The activity of cdk5 is regulated by its binding with neuron-specific activator proteins p35, p25, and p39. Cleavage of p35 to the more stable proteolytic fragment p25 is increased in AD brain, leading to subsequent upregulation of cdk5 activity (Lee et al., 1999; Patrick et al., 1999; Tseng et al., 2002). An increasing number of in vitro studies have shown that cdk5 is capable of phosphorylating tau at several epitopes of relevance to AD (Michel et al., 1998; Patrick et al., 1999; Alvarez et al., 2001; Lund et al., 2001; Gotz and Nitsch, 2001; Bu et al., 2002; Hashiguchi et al., 2002; Liu et al., 2002). Furthermore, an inhibitor of cdk5 activity has been shown to reduce tau hyperphosphorylation and neuronal degeneration in vivo (I. Vincent et al., 2002, SFN, Program No. 318.11). Transgenic mouse models with elevated cdk5 activity have abnormalities of tau and other cytoskeletal components which leads to the accumulation of phosphorylated tau and neurofilaments in spheroids and the development of axonopathy (Ahlijanian et al., 2000; Bian et al., 2002). These mice do not, however, develop tau aggregates or NFTs, suggesting that cdk5-mediated phosphorylation of tau does not initiate AD-type neurofibrillary pathology. To assess whether increased cdk5 activity affects the progression of tau pathology, we crossed mice with enhanced endogenous cdk5 activity to mice with mutant human tau. Double transgenic mice showed enhanced hyperphosphorylation and aggregation of tau, and increased tangle formation compared to single transgenic tau mice. Cdk5 may act directly, indirectly, or in concert with GSK3 as this kinase was also overactive in the double transgenic mice, and colocalized with both aggregated tau and cdk5. This study shows that although previous studies suggest activation of cdk5 is not sufficient to initiate tangle formation in mice, increased activity of cdk5 greatly enhances neurofibrillary pathology development. Thus inhibitors of cdk5 activity may have utility in ameliorating the pathology of AD.

Results

P25 Overexpression Is Associated with Enhanced Cdk5 Activity

P25 transgenic mice were derived from mice overexpressing the human p25 cDNA in neurons (Ahlijanian et al., 2000). Hemizygous mice were crossed with mice expressing mutant human tau (P301L, 4R0N) (Lewis et al., 2000) and progeny were genotyped as tau (T), p25, p25/T double transgenic, and nontransgenic (Ntg).

Alteration in the ratio of p25:p35 through increased production of the activator p25 is associated with enhanced cdk5 activity in humans (Lew et al., 1994). Transgenic mice overexpressing either p35 or p25 have been created to attempt to enhance the in vivo activity of cdk5, but only the p25 mice have an obvious phenotype (Ahlijanian et al., 2000; Bian et al., 2002). In general, p25 overexpression in mice enhanced cdk5 activity 2- to 5-fold. Although there was no hyperphosphorylation of

*Correspondence: duff@nki.rfmh.org

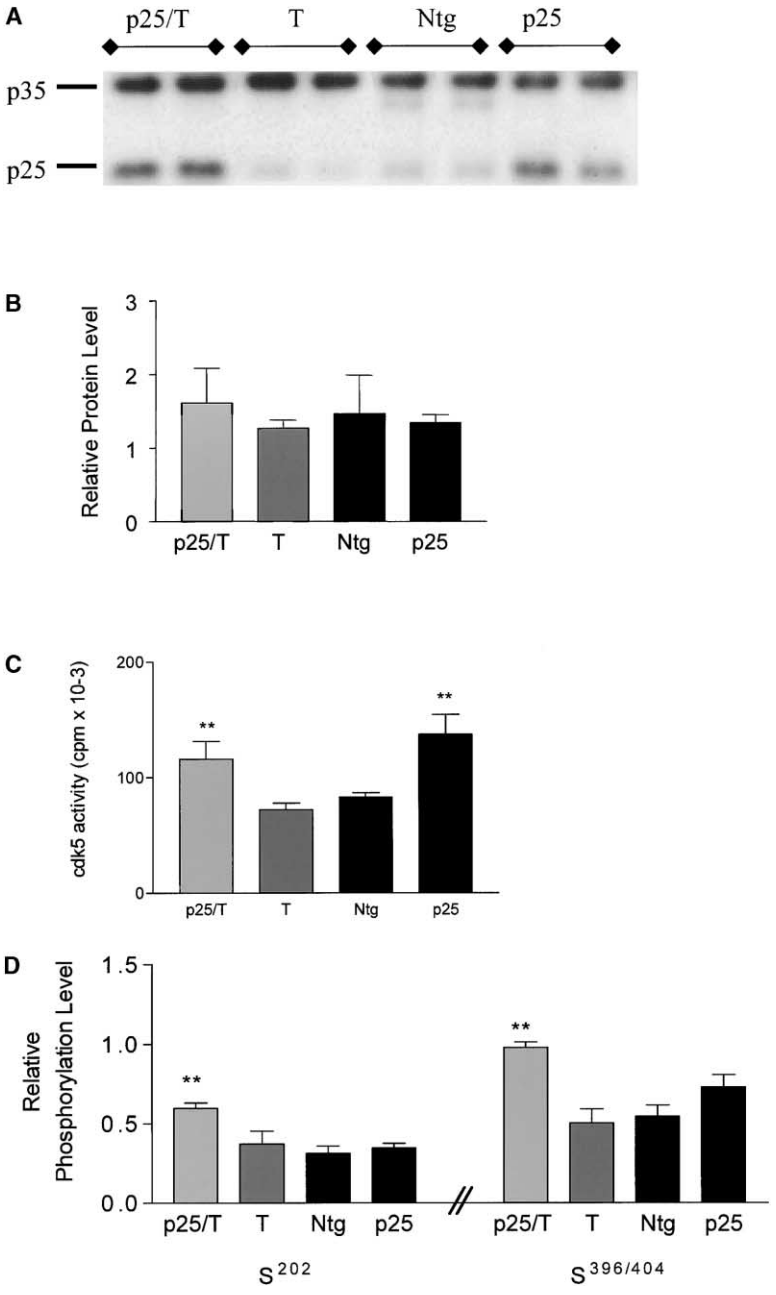

Figure 1. P25 Expression, Cdk5 Activity, and Tau Hyperphosphorylation in p25/T Mice

Western blot analysis showing p35 and p25 expression in p25/T, T, p25, and Ntg mice. P25 expression was greatly increased relative to p35 in p25 transgenic animals (A). Western blot analysis of cdk5 levels in the amygdala showed that p25 transgenic animals did not show a higher level of cdk5 when compared to littermate controls (B). Kinase activity assays showed an approximately 2-fold increase in cdk5 activity in the amygdala of p25 transgenic mice (C) (p25/T versus T and p25 versus Ntg). Tau ELISA (D) showed hyperphosphorylation of tau in the amygdala of p25/T mice compared to T at epitopes S^{202} and $S^{396/404}$. There was no significant increase in the relative phosphorylation level in p25 single transgenics compared to Ntg mice. **$p < 0.005$; $n = 5–8$ in all analyses.

tau, tau was phosphorylated at several sites in select neurons, and axonopathy and tau accumulation in the form of spheroids resulted, especially in the amygdala. Although early generations of p25 mice supplied to us developed spheroids, p25 mice in this study had lost the spheroid phenotype, presumably due to genetic drift. Western blot analysis of p35/p25 levels showed that as expected, p25 was significantly enhanced in transgenic mice expressing the p25 transgene (Figure 1A), but p35 levels were unchanged. Immunoblotting with anti-cdk5 antibodies showed that the level of cdk5 in the same region (amygdala) of p25 overexpressing mice (p25/T and p25) was not altered when compared to controls (Ntg and T mice, Figure 1B). However, kinase activity assays demonstrated that cdk5 activity in this area was increased approximately 2-fold ($p < 0.05$; Figure 1C) in the same mice. P301L transgene overexpression and the phenotype it confers is not associated with altered cdk5 activity, as there was no significant difference in activity levels between single transgenic P301L mice and nontransgenic littermates (T versus Ntg) or between p25/T mice and single transgenic p25 mice (p25/T versus p25). Endogenous tau in p25 mice was not hyperphosphorylated compared to Ntg mice in total brain homogenate from this region, as demonstrated previously by immunoblot analysis of this line (Ahlijanian et al. 2000). There was, however, a trend to increase, especially for tau phosphorylated at $S^{396/404}$ (Figure 1D).

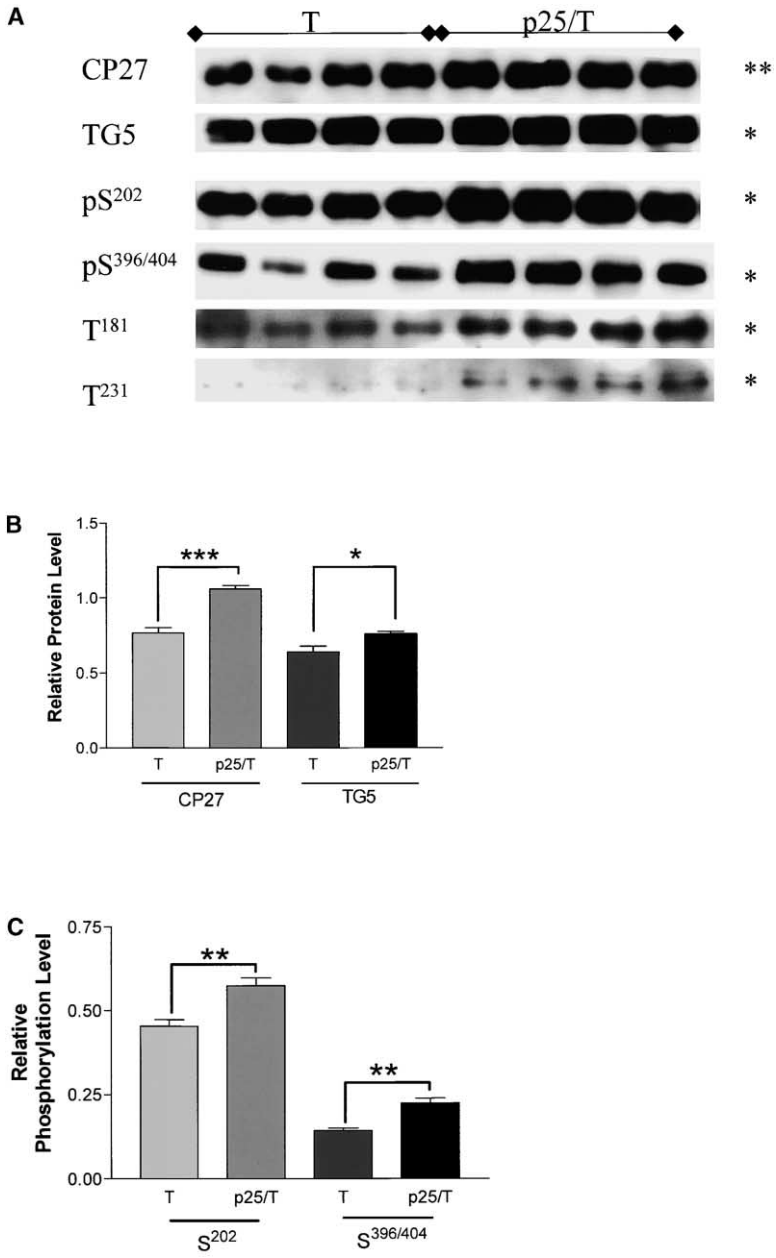

Figure 2. Analysis of Heat Stable Tau

There was a significant increase in the amount of total human (CP27) and mouse/human (TG5) in p25/T mice compared to T (A). Hyperphosphorylation was observed at cdk5-directed sites S^{202}, $S^{396/404}$, T^{181}, and T^{231} in p25/T when normalized to CP27 levels. ELISA analysis of total tau levels confirmed the Western blot analysis for total tau levels (B) and phospho-tau (C). These data suggest that cdk5 phosphorylates free, unaggregated tau. ***$p < 0.0005$, **$p < 0.005$, *$p < 0.05$; n = 5–8 in each group.

Enhanced Cdk5 Activity Is Associated with Increased Tau Hyperphosphorylation in p25/T Mice

In heat-stable tau preparations, antibodies recognizing both human tau (CP27) and total tau (mouse/human, TG5) showed an increase in tau in p25/T mice compared to T mice ($p < 0.005$ for CP27, $p < 0.05$ for TG5) when assessed by immunoblot (Figure 2A) and ELISA (Figure 2B). Phosphorylation of tau was enhanced at putative cdk5-directed sites S^{202}, $S^{396/404}$, T^{181}, and T^{231} (Liu et al., 2002; Hashiguchi et al., 2002) in p25/T mice relative to T (Figure 2A). When normalized to either CP27 or TG5, there was a significant increase in phosphorylation (hyperphosphorylation) at these sites ($p < 0.05$ for all). ELISA confirmed the results of immunoblot analysis (Figure 2C).

Cdk5 Overactivity Is Associated with Increased Aggregation of Tau in p25/T Mice

We next examined whether cdk5 overactivity promoted aggregate formation in two regions, the cortex and the hindbrain. Three fractions were prepared: total lysate after a low-speed spin (LSS) which contains all proteins, supernatant after addition of sarkosyl and a high-speed spin (HSS), and the sarkosyl-insoluble pellet (SP) which is highly enriched for aggregated tau.

Immunoblot and ELISA analysis was performed on the LSS (Figure 3) and SP (Figure 4) fractions. Quantitative analysis of LSS showed an increase ($p < 0.05$) in human tau in the brainstem by immunoblotting (Figure 3A) and ELISA (Figure 3C), but not the cortex of p25/T mice compared to T mice (Figures 3B and 3C). When normalized to human tau, there was a significant increase in

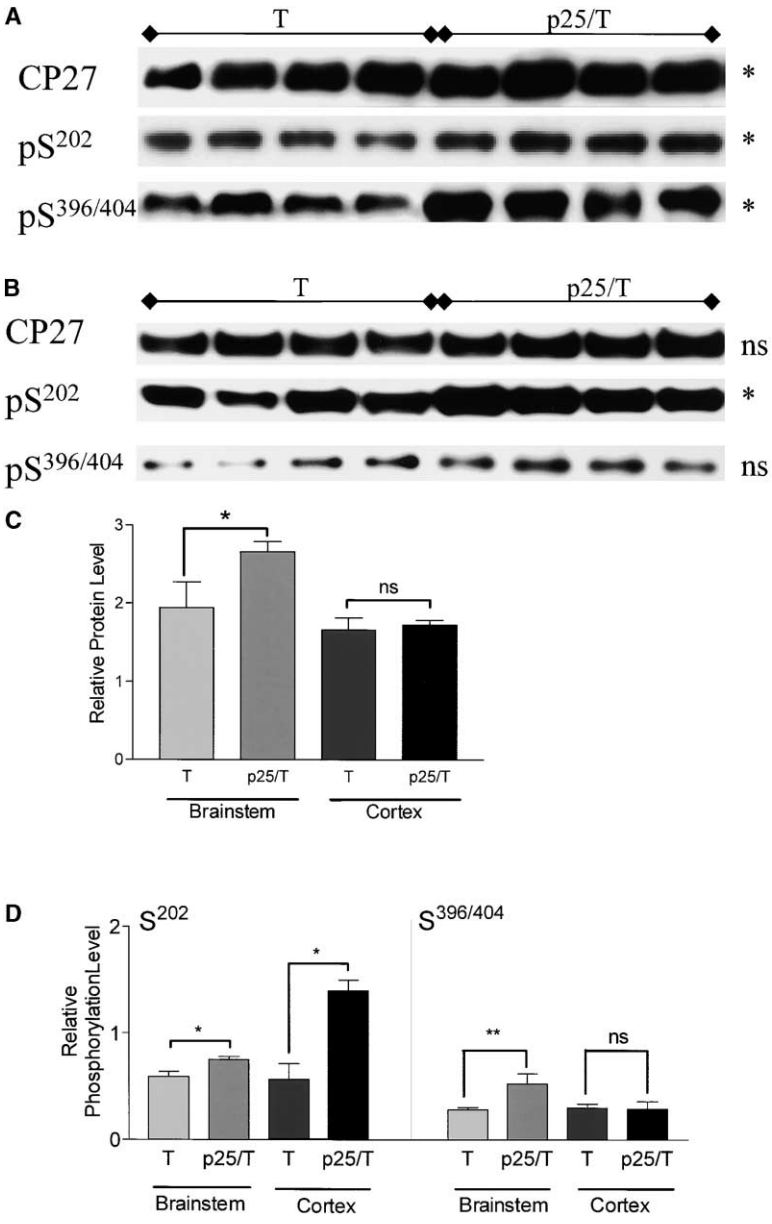

Figure 3. Regional Hyperphosphorylation of Tau in p25/T Mice

Levels of total and phosphorylated (S^{202} and $S^{396/404}$) tau were increased in the brainstem lysate from p25/T mice when assessed by immunoblotting (A). There was no increase in total tau levels in the cortex (B), with hyperphosphorylation detected only at S^{202}, suggesting that the brainstem hyperphosphorylation is more advanced. The increase in total tau was also significant in the brainstem, but not the cortex when assessed by ELISA (C). When ELISA data was normalized to levels of total tau (CP27), S^{202} was significantly hyperphosphorylated in the brainstem and cortex of p25/T mice, while phosphorylation at $S^{396/404}$ was only significantly increased in the brainstem (D). $^{**}p < 0.005$; $^{*}p < 0.05$; ns, $p > 0.05$; $n = 5–8$ in each group.

tau hyperphosphorylated at S^{202} in p25/T mice relative to T mice in both the brainstem and cortex ($p < 0.05$ for both; Figures 3A, 3B, and 3D). In the brainstem of p25/T mice, there was also a significant increase in tau hyperphosphorylated at $S^{396/404}$ compared to T mice ($p < 0.05$; Figures 3A and 3D), but this was not seen in the cortex ($p > 0.05$; Figures 3B and 3D).

Tau from the sarkosyl pellet is regarded as filamentous, aggregated, and synonymous with that identified by immunohistochemistry in NFTs. To confirm this, we identified phospho-$S^{396/404}$ immunoreactive filaments in the brainstem SP of both p25/T and T mice by immunogold labeling and electron microscopy (Figure 4A). No qualitative differences were identified in tau filaments from the two mouse groups. Filaments identified were very similar to those described previously in the tau P301L mouse—mainly straight, with a diameter of between 10 and 30 nm (Lewis et al., 2000). Quantitative immunoblotting and ELISA showed that aggregated, human tau was significantly increased in the SP of brainstem and cortex from double transgenics ($p < 0.005$, $p < 0.05$, respectively; Figures 4B–4G). No tau was identified in the SP fraction from p25 or Ntg animals (data not shown). Both p25/T and T mice had tau in the SP that migrated at approximately 53 kDa. Tau from p25/T mice had an additional form that migrated at approximately 64 kDa (Figures 4B and 4C, arrows). The lower mobility band was highly immunoreactive with CP13 (S^{202}) in the brainstem (Figure 4B), whereas the 53 kDa was the predominantly labeled band in the cortex, with a small amount of the 64 kDa band being visible (Figure 4C). Overall, there was a significant increase in pS^{202} tau in the SP of the brainstem assessed by immunoblotting and ELISA (Figures 4B and 4D).

Phospho-$S^{396/404}$ was detected in both bands in the brainstem and cortex of p25/T mice (Figures 4B and

4C), but there was relatively little of the 64 kDa tau isoform in the brainstem of T mice. Both assessment methods showed a significant difference for $S^{396/404}$ in the brainstem of the p25/T mice compared to T (Figures 4B and 4D), but not in the cortex (Figures 4C and 4E), although the contribution of the 64 kDa form of phosphorylated tau could only be appreciated on the immunoblot. When the amount of aggregated, phospho-tau in the SP was normalized to the amount of tau in the LSS, there was a striking increase in the proportion of tau aggregated in the brainstem of p25/T mice compared to T controls (Figure 4F). In the brainstem of p25/T mice, the increased phosphorylation observed in the proportion of tau that has aggregated reflects the greater proportion of lower mobility tau (64 kDa band). The effect of p25/cdk5 on aggregation in the cortex was not as profound. Although the proportion of total aggregated tau was increased in p25/T mice (Figure 4G), it was not significantly more hyperphosphorylated. However, it is clear from the immunoblots that a proportion of the phospho-tau aggregated in the cortex of p25/T mice has undergone a mobility shift not observed in the T mice. The reciprocal results were observed in the HSS (data not shown), with reduced levels of sarkosyl-soluble, unaggregated, hyperphosphorylated tau observed in p25/T mice.

Both Cdk5 and GSK3 Are Associated with Aggregated Tau in the Brainstem

We previously showed that the level of cdk5 was unchanged in p25/T mice compared to T controls, whereas its activity was significantly increased (Figures 1B and 1C). Similarly, we have also determined that the protein level of GSK3α/β was unchanged, but its activity was increased in total lysate from p25/T mice compared to T controls (Figure 5A). We next examined total and active forms of cdk5 and GSK3 associated with aggregated tau in the brainstem SP fraction of p25/T and T mice (Figure 5B). Total and active forms of cdk5 were associated with aggregated tau from p25/T and T mice. GSK3 and its activated forms, especially the GSK3α and β2 isoforms, were also identified in the SP fraction from p25/T mice, but they were negligible in aggregated tau preparations from T mice (Figure 4B). The presence of these kinases in the SP fraction indicates that both of these kinases are strongly bound with tau that is aggregated. Confocal microscopy was performed to demonstrate that the activated kinases colocalize with tau in neurons (Figure 5C). Phospho-GSK3 (Figure 5C, green) colocalized with human tau in its abnormal AD-relevant conformation (recognized by MC1, red) mainly in the cell body (overlap shown in yellow), although some processes were also immunolabeled. Cdk5 and tau also overlapped throughout the soma, and processes were prominently labeled. We were also able to show a degree of colocalization between cdk5 and GSK3α/β in neurons.

Overactivity of Cdk5 Enhances the Development of NFTs in p25/T Mice

Female tau P301L mice at 12 months of age have been shown to develop neuronal cell body staining for phospho-tau (pS^{202} and $pS^{396/404}$) and for conformationally abnormal tau mainly in the spinal cord and brainstem regions, but also to some extent in the amygdala. Immunopositive neurons were only occasionally found in the cortex. NFTs were identified by Thioflavin S and Gallyas silver stain mainly in the spinal cord (Lewis et al., 2000). To assess whether doubly transgenic p25/T mice derived from this line had increased numbers of NFTs in addition to increased hyperphosphorylated, aggregated tau as a result of elevated kinase activity, the number of Gallyas silver-positive neurons in the brainstem of p25/T and T mice were counted. We found a highly significant increase in the number of NFTs in the brainstem of p25/T mice relative to T controls (Figure 6; $p < 0.05$), which correlates with the results of the biochemical analyses. Gallyas-positive neurons were not found in p25 or Ntg mice (data not shown).

Discussion

The most striking finding of this study was the dramatic increase in sarkosyl-insoluble, hyperphosphorylated, aggregated tau in double transgenic mutant tau mice with enhanced endogenous cdk5 activity, compared to age, stage, and gender-matched tau mutant mice with normal activity of cdk5. The use of a transgenic mouse with increased levels of the activator p25 that has normal levels, but enhanced activity of endogenous cdk5, makes this a particularly good in vivo system in which to study the impact of cdk5 in initiating events involved in enhancing pathogenesis.

We have shown that tau is hyperphosphorylated at several sites including S^{202}, T^{181}, T^{231}, and $S^{396/404}$ in heat-stable tau preparations from p25/T mice. As these preparations are free of tau aggregates, this suggests that cdk5, or downstream kinases, can phosphorylate tau prior to, or independently of, aggregation. Aberrant phosphorylation at the sites identified has been suggested to lead to a significant reduction in the affinity of tau for microtubules, and its ability to stabilize them (Biernat et al., 1993; Sengupta et al., 1998). The reduced affinity of phosphorylated tau for microtubules could increase the amount of unbound cytoplasmic tau as shown by the increased levels of CP27 and TG5. In vivo, phosphorylated tau polymerizes faster than it can be degraded (Billingsley and Kinkaid, 1997), which may also account for the increase in total tau we have observed. Once unbound tau reaches a critical level, it is more prone to fibrillization, which would encourage the increased aggregation we have demonstrated in the p25/T mice. This is supported by previous studies which have shown that tau hyperphosphorylation promotes the self-assembly of filamentous tau (Alonso et al., 2001). Interestingly, we have also found activated kinases in association with aggregated tau, suggesting that these kinases continue to phosphorylate tau once tangle formation has begun. These findings are in agreement with previous immunohistochemical studies which have shown a strong association between NFTs, cdk5, and/or GSK3β (Baumann et al., 1993; Paudel et al., 1993; Yamaguchi et al., 1996; Pei et al., 1997).

The increase in aggregated tau in the brainstem region of p25/T mice was more pronounced than in the cortex, most likely due to the high level of human tau expression, and/or increased vulnerability of this region reported for

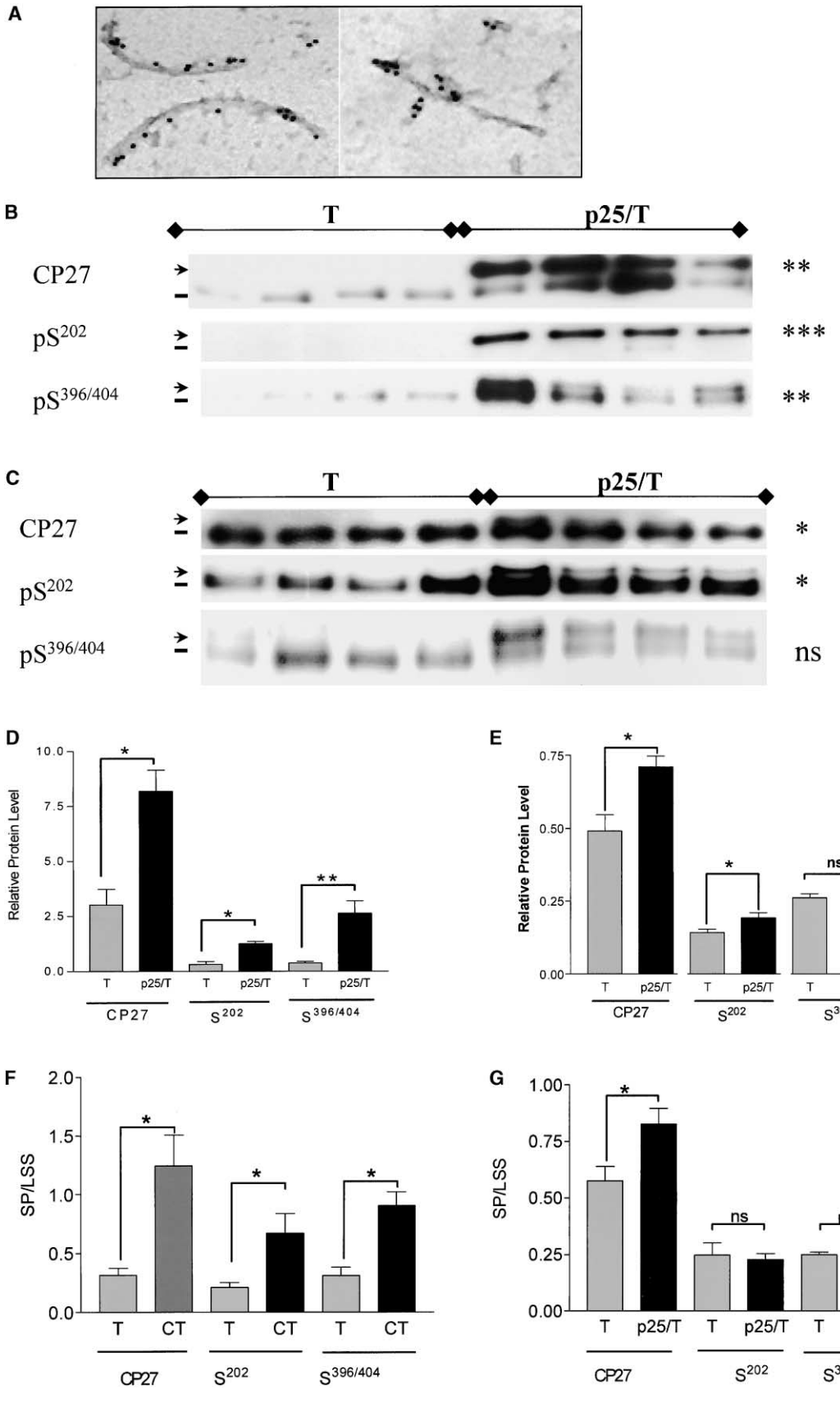
A
B
T
p25/T
CP27
pS202
pS396/404
**
***
**
C
T
p25/T
CP27
pS202
pS396/404
*
*
ns
D
Relative Protein Level
10.0
7.5
5.0
2.5
0.0
*
*
**
T
p25/T
CP27
S202
S396/404
E
Relative Protein Level
0.75
0.50
0.25
0.00
*
*
ns
CP27
S202
S396/404
F
SP/LSS
2.0
1.5
1.0
0.5
0.0
*
*
*
T
CT
CP27
S202
S396/404
G
SP/LSS
1.00
0.75
0.50
0.25
0.00
*
ns
ns
T
p25/T
CP27
S202
S396/404

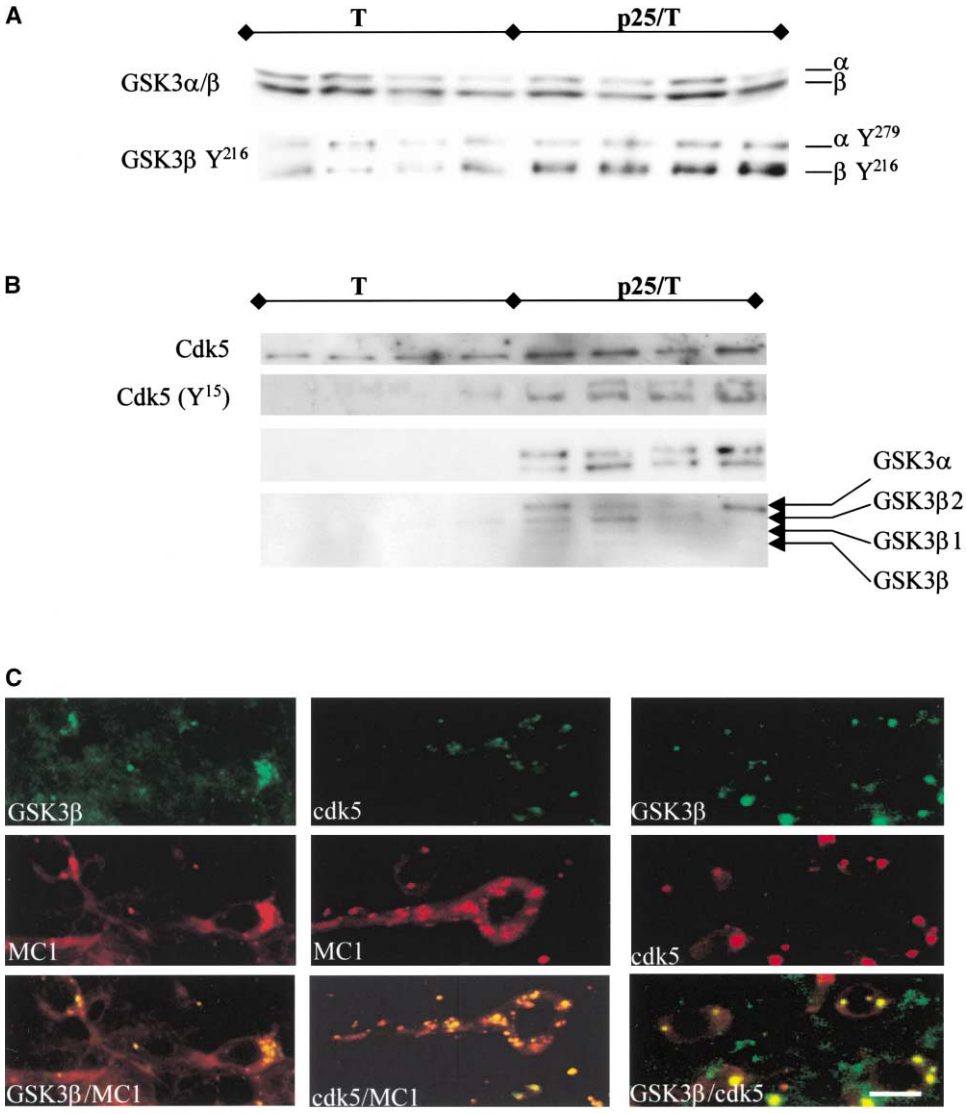

Figure 5. Association of Cdk5 and GSK3 with Aggregated Tau

Western blot analysis of GSK3 levels in total lysate. There was no increase in the total protein level of GSK3 α or β, but the active form of GSK3β (Y^{216}), but not gsk3α (Y^{279}), was increased in p25/T mice (A). Both cdk5 and GSK3 and their active forms were detected in association with aggregated tau (B). Cocal microscopy demonstrated colocalization of the active forms of these kinases with MC1-positive tau, and colocalization of cdk5 and GSK3β with each other (C). Scale bar, 50 μm.

the parental tau P301L mouse line (Lewis et al., 2000). The brainstem appeared to be at a later stage in pathology progression as indicated by the presence of higher molecular weight tau forms and the increase in tau hyperphosphorylated at $S^{396/S404}$. Hyperphosphorylation at T^{181}, S^{202}, and T^{231} are thought to be early events in NFT formation, indicative of the presence of pretangle tau, whereas $S^{396/404}$ hyperphosphorylation occurs later (Augustinack et al., 2002). Brain regions without motor neurons (e.g., cortex) also have increased hyperphosphorylated/aggregated tau compared to the single tau transgenics, suggesting that tangle distribution does shift (or extend) in the double transgenics.

In the mice studied, enhanced brainstem neurofibril-

Figure 4. Cdk5 Enhances Tau Aggregation

Immunogold staining of EM sections (21,000× magnification) showing tau filaments immunoreactive with PHF1 were present in the sarkosyl pellet (A). The level of sarkosyl-insoluble, aggregated tau was increased in both the brainstem (B) and cortex (C) of p25/T mice when assessed by immunoblotting. Tau forms of 53 kDa (line) and 64 kDa (arrow) were observed. When assessed by ELISA, there was a significant increase in total tau and tau phosphorylation at S^{202} in the brainstem (D) and cortex (E) and at $S^{396/404}$ in the brainstem alone (D). The proportion of aggregated tau:total tau was greatly increased in p25/T mice in both brainstem (F) and cortex (G). ***$p < 0.0005$; **$p < 0.005$; *$p < 0.05$; ns, $p > 0.05$; $n = 5$–10 in each group.

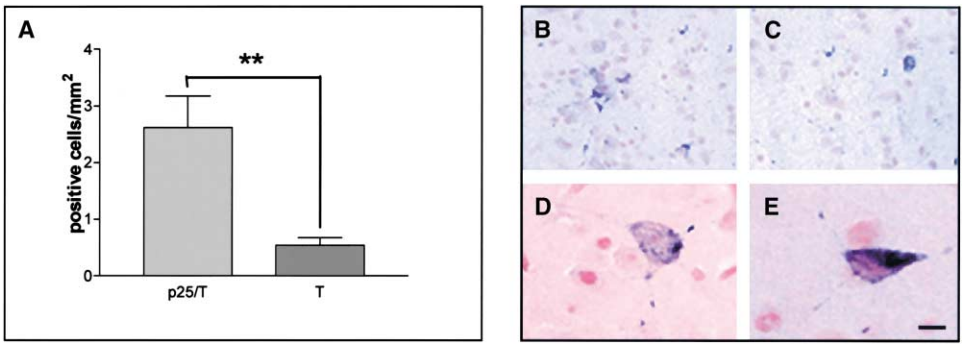

Figure 6. Cdk5 Enhances the Development of Neurofibrillary Pathology

Quantitative analysis of the number of Gallyas silver-stained neurons in the brainstem of p25/T and T mice showed a 3- to 4-fold increase in the number of tangles in double transgenic p25/T mice compared to matched T controls (A). Typical brainstem area in p25/T mice (B) and representative section from T mice brainstem (C). Higher power images showing Gallyas-stained neurofibrillary tangles present in p25/T mice are shown in (D) and (E). Scale bar, 10 μm (B and C) and 50 μm (D and E); **$p < 0.005$; $n = 7–10$ in each group.

lary pathology in p25/T mice was not associated with significantly accelerated dystonia (Lewis et al. 2000) that normally starts in tau P301L-derived mice at 12–14 months of age (data not shown). Both p25/T and T mice used in this study were matched in terms of their stage of dystonia, with both groups being considered unaffected, or marginally affected when assessed for degree of paralysis (data not shown). It is possible that any acceleration in outwardly visible degeneration was too subtle to be identified in this study, but mice aged beyond 1 yr are not yet available.

Studies have implicated cdk5 as a candidate kinase for early tau hyperphosphorylation due to its axonal localization (Ishiguro et al., 1995). Inhibition of cdk5 activity specifically inhibits fast anterograde axonal transport and redistribution of cellular proteins (Ratner et al., 1998). GSK3β is thought to be associated with neurofibrillary changes (Yamaguchi et al., 1996; Pei et al., 1997; Planel et al., 2002), particularly in later-stage phosphorylation of tau as this kinase is associated with microtubules in the cell body, which would bring it into contact with tau once it has redistributed to the somatodendritic portion of the cell (Flaherty et al., 2000). In the p25/T mice, overactivity of cdk5 over a long period of time could not only enhance the redistribution of tau into the cell body which occurs in tau overexpressing mice, but also increase the "priming" of tau for subsequent phosphorylation by GSK3β (Ishiguro et al., 1995; Sengupta et al., 1997). The colocalization of active cdk5 and tau in the soma and processes, and GSK3β and tau mainly in the soma of our mice, supports this idea and is consistent with tau/kinase observations in other tau transgenic mice (Yamaguchi et al., 1996; Pei et al., 1997; Flaherty et al., 2000; Gotz and Nitsch, 2001). We have also shown that cdk5 and GSK3α/β colocalize within neurons of our mice, and it is likely that both kinases, together with other putative tau kinases, are involved in NFT formation and/or progression (Veeranna et al., 2000; Gotz and Nitsch, 2001; Williamson et al., 2002). We have determined that both active cdk5 and GSK3β are associated with tau in an abnormal conformation (MC1 immunoreactive) by immunohistochemistry, and that both active and inactive kinases are associated with aggregated tau fractions, supporting the theory that a macromolecular complex of kinases, substrates, and regulators is present in tangle-bearing neurons.

Although both cdk5 and GSK3β are known to phosphorylate murine tau in p25 or GSK3β overexpressing transgenic mice respectively, no increase in insoluble tau aggregates or tangles were observed, although there was evidence of axonal dysfunction (Ahlijanian et al., 2000; Spittaels et al., 2000; Lucas et al., 2001; Bian et al., 2002). This suggests that in mice, low-level phosphorylation of axonally distributed, normal tau is not sufficient to initiate tangle formation. Confusingly, in a double transgenic human tau/GSK3 overexpressing mouse, axonal pathology and spheroids were decreased compared to the single transgenic tau control (Spittaels et al., 2000), but aggregated tau formed in the omatidia of a double transgenic, human tau/GSK3 overexpressing *Drosophila* model (Jackson et al., 2002). The significant differences between all these models in terms of species/strain (mouse, fly), kinase type and distribution (cdk5, GSK3, processes, or cell body), tau type and distribution (endogenous murine tau or human tau overexpressor, axonal, or somatodendritic distribution), and cell type (motor neurons, cortical/hippocampal neurons, or sensory neurons) makes it difficult to extrapolate the relevance of the results to human tau pathogenesis. In terms of the contribution of cdk5 to pathogenesis in a mouse model with tangles that are highly relevant to human tauopathy, we have provided compelling evidence that cdk5 overactivity can promote tau aggregation and tangle formation, with concomitant hyperphosphorylation, thereby enhancing the development of neurofibrillary pathology in mice predisposed to tauopathy. The p25 mice do not have insoluble tau nor do they have Gallyas silver-stained neurons (data not shown), so the phenotype seen in the p25/tau mice is not the result of overlain pathologies, but interactive pathways. Importantly, this occurs both in the brainstem, and in cortex—a region not usually affected in tau P301L mice that is of significant importance in dementing diseases.

The neuropathology of AD is characterized not only by NFTs but also by extracellular amyloid plaques composed mainly of aggregated Aβ peptides. Several studies have shown that Aβ influences tau kinase activity in

vitro (Takashima et al., 1993; Tomidokoro et al., 2001; Rank et al., 2002), and Town et al. (2002) describe a mechanism whereby Aβ induces tau hyperphosphorylation via the cdk5 pathway. It has been shown that calpains (which increase cdk5 activity by increasing cleavage of p35 to p25) are upregulated in AD brain (Grynspan et al., 1997; Tsuji et al., 1998; Lee et al., 2000), and recent studies have shown that elevated Aβ enhances tangle formation in mutant tau mice (Lewis et al., 2001; Gotz et al., 2001). This suggests that the induction of signal transduction pathways by Aβ enhances neurofibrillary pathology, although this may only occur in mice predisposed to it. Neither our study nor other in vivo studies using the P301L mice show causality or initiation of pathogenesis as the mice start life with abnormal tau, but the data suggest that intervention using kinase inhibitors may at least ameliorate the progression of neurofibrillary pathology in diseases such as AD.

Experimental Procedures

Transgenic Mice

P25 transgenic mice overexpress the human p25 gene under the control of the NSE promoter (Ahlijanian et al., 2000). JNPL3 transgenic mice with the $Pro^{301} \rightarrow$ Leu (P301L) tau mutation develop NFTs in the basal telencephalon, diencephalon, brainstem, and spinal cord, along with neuronal loss that is most evident in the spinal cord (Lewis et al. 2000). Hemizygous p25 and JNPL3 (tau P301L) mice were crossed and progeny were genotyped as tau (T), p25, p25/tau (p25/T), and nontransgenic (Ntg). Mice were matched for degree of postural dystonia, and only those graded as preparalysis/early stage degeneration were selected for analysis. Female mice at 12 months of age (n = 5–8) from each genotype were used for ELISA and immunoblot analysis. Mice were sacrificed by cervical dislocation, and tissue was dissected into brainstem, amygdala/hippocampus, and cortex. Tissue was immediately snap frozen on dry ice.

Antibodies

The following monoclonal antibodies were used and specificity, isotype and source are given in parentheses: human tau: CP27 (mouse IgG2b; P.D.), TG5 (220–240, mouse IgG1; P.D.); phospho-tau: CP13 (Ser-202, mouse IgG1; P.D.), PHF1 (Ser-396/404, mouse IgG1; P.D.), T^{231} (Thr-231, rabbit IgG; Biosource International, Camarillo, CA), T^{181} (Thr-181, rabbit IgG; Biosource); conformation-dependent tau: MC1 (5-15, 312-322, mouse IgG1; P.D.), TG3 (Ser-231, mouse IgM; P.D.); and kinases: p35 (p35 C-19, rabbit IgG; Santa Cruz Biotechnologies), cdk5 (cdk5 C8, rabbit IgG; Santa Cruz Biotechnologies, Santa Cruz, CA), cdk5 pY^{15} (phosphotyrosine 15 of cdk5, goat IgG; Santa Cruz Biotechnologies), GSK3a/b (gsk3α/β, mouse IgG; Biosource), phospho-GSK3β (phosphotyrosine 216 of GSK3β, rabbit IgG; QCB, Hopkinson, MA.).

Immunoprecipitation and Cdk5 Activity Assay

Immunoprecipitation and kinase assays were performed on mouse amygdala using the NF-H-derived 14-mer peptide with two KSPXK repeats as enzyme substrate as described in Veeranna et al. (1996, 1998). Briefly, the assay was performed in a total volume of a 50 μl reaction mixture containing 50 mM Tris-HCl (pH 7.4), 5 mM $MgCl_2$, 1 mM vanadate, 1 mM EGTA, 1 mM EDTA, 1 mM DTT, 1 mM [γ-^{32}P]ATP, and 0.2 mM peptide substrate plus 0.1 μM okadaic acid or 0.1 μM microcystin LR and 10 μl of enzyme. The reaction was initiated by the addition of [γ-^{32}P]ATP, incubated at 30°C for 2–4 hr, and terminated by transferring an aliquot onto P81 phosphocellulose squares.

Semiquantitative Analysis of Phosphorylated Tau

Tissue regions were homogenized using a polytron homogenizer at a w/v ratio of 100 mg tissue/ml of 50 mM Tris-buffered saline (TBS), pH 7.4, containing 2 mM EGTA, 1 mM PMSF, 10 mM sodium fluoride, and 1 mM sodium orthovanadate. The homogenates were centrifuged at 15,000 × g for 20 min, and resultant supernatants were used for the assay. Protein concentration was determined and adjusted to 0.7 μg/μl. Protein samples were serially diluted, and 50 μl of diluted sample was applied to a coated Maxi-Sorb ELISA plate (Nalgene, Nunc International, Roskilde, Denmark). After samples were evaporated to dryness, the plates were blocked in TBS containing 5% nonfat dry milk for 1 hr at room temperature. Tau antibodies were used at 1:200 dilution and were incubated overnight at 4°C. Plates were washed with 50 mM TBS containing 0.5% Tween 20 × 5. Bound antibodies were detected using HRP-coupled secondary antibodies and visualized using a kit (TMB Microwell Peroxidase Substrate System; Kirkengaard & Perry Laboratories, Gaithersburg, MD). O.D. was calculated using a Bio-Kinetics Reader EL312e (Bio-Tek Instruments, Winooski, VT). The hyperphosphorylation status of tau was calculated by normalizing the amount of phosphorylated to the amount of total tau.

Immunoblot Analysis of Heat Stable Tau

Mouse amygdala samples were homogenized with a polytron homogenizer on ice at a w/v ratio of 100 mg tissue/ml in 50 mM Tris, pH 7.4, 0.8 M NaCl, and 5% β-mercaptoethanol. Heat-stable fractions were prepared according to the method described in Duff et al. (2000). Samples containing 1–3 μg of protein were run on a 12% Tris-tricine gel (Invitrogen, Carlsbad, CA), then electrophoretically transferred to PVDF membrane. After blocking with 5% dry milk for 1 hr, membranes were probed with primary antibodies, detected using HRP-coupled secondary antibodies and visualized by enhanced chemiluminescence reagent (SuperSignal West Pico; Pierce).

Immunoblot Analysis of Aggregated Tau

Sarkosyl extractions were performed on mouse brainstem or cortex samples according to the method of Greenberg and Davies (1990). Total brain lysate (LSS), sarkosyl-soluble (HSS), and insoluble (SP) fractions were analyzed. Samples were separated on 16% Tris-tricine gels and electrophoretically transferred to PVDF membrane. Membranes were blocked in PBS containing 5% nonfat dry milk, then probed with antibodies against tau and tau kinases. Bound antibodies were detected using HRP-coupled secondary antibodies (Southern Biochemicals) and were visualized by enhanced chemiluminescence (Pierce).

Electron Microscopy

Sarkosyl-insoluble tau was resuspended in sterile, filtered 10 mM TBS for EM. 5 μl sample was placed on Formvar-carbon-coated 300 mesh nickel grids for 2 min and rinsed in ddH_2O. After drying, grids were washed for 2 min in a solution of PBS/0.1% BSA/0.1% gelatin, then blocked in PBS buffer containing 5% normal goat serum for 10 min. Grids were incubated in phospho-tau antibody for 60 min at room temperature and washed. Primary antibody was detected with gold-tagged anti-mouse IgG secondary antibody (1/25). Samples were fixed in 2% glutaraldehyde, washed, and stained with 3% aqueous uranyl acetate. The grids were examined on a Phillips CM10 electron microscope at 80kV.

Gallyas Silver Stain

Mice were killed by cervical dislocation without perfusion, and tissue was drop fixed in 4% paraformaldehyde in 100 mM phosphate-buffered saline (pH 7.4) for 18 hr, followed by cryoprotection in 15% sucrose with 0.5% sodium azide overnight. Serial 30 μm sections were cut using a freezing sledge microtome (Leica T2400). Silver staining was performed according to the protocol of Gallyas modified by Braak (Braak et al., 1988). Briefly, sections were rehydrated and placed in periodic acid (5%) for 5 min. Following washing, slides were stained in alkaline silver iodide for 1 min, followed by washing in acetic acid (0.5%) and were then developed (4–10 min). Slides were then washed and placed in gold chloride (0.1%) for 2 min and sodium thiosulphate (10%) for 2 min. Following counterstaining in nuclear fast red (0.1%), slides were dehydrated and mounted. The number of positively stained cells in equivalent brainstem regions were counted, and results were expressed as number of positive cells/mm^2 (Bancroft and Stevens, 1990).

Immunofluorescence

Tissue sections were prepared as described previously and incubated with monoclonal MC1 and either polyclonal cdk5 pY^{15}or gsk3β pY^{216} primary antibodies. Fluorophore-tagged anti-mouse IgG (Texas red) and anti-rabbit IgG (FITC) were used to detect MC1 and cdk5 respectively. Samples were viewed with a Leica DM 1 RBE confocal microscope (Leica Camera AG, Solms, Germany). Images were acquired with a UV 40× 1.25 NA oil PL AP01 objective (Leica) with pinhole settings at ~1 airy unit for all images.

Acknowledgments

The authors would like to thank Emmanuel Planel at Riken Institute for helpful discussions and expert advice. We wish to thank Mike Hutton and Jada Lewis at Mayo Clinic, Jacksonville, FL for P301L mice and Linda Rousseau for help with silver staining. Cori Peterhoff at NKI is thanked for assistance with confocal microscopy. This work was supported by a PO1 grant AG 172116 from NIA to K.D. and D.D.

Received: November 14, 2002
Revised: February 25, 2003
Accepted: April 17, 2003
Published: May 21, 2003

References

Ahlijanian, M.K., Barrezueta, N.X., Williams, R.D., Jakowski, A., Kowsz, K.P., McCarthy, S., Coskran, T., Carlo, A., Seymour, P.A., Burkhardt, J.E., et al. (2000). Hyperphosphorylated tau and neurofilament and cytoskeletal disruptions in mice overexpressing human p25, an activator of cdk5. Proc. Natl. Acad. Sci. USA *97*, 2910–2915.

Alonso, A., Zaidi, T., Novak, M., Grundke-Iqbal, I., and Iqbal, K. (2001). Hyperphosphorylation induces self-assembly of tau into tangles of paired helical filaments/straight filaments. Proc. Natl. Acad. Sci. USA *98*, 6923–6928.

Alvarez, A., Munoz, J.P., and Maccioni, R.B. (2001). A Cdk5-p35 stable complex is involved in the beta-amyloid-induced deregulation of Cdk5 activity in hippocampal neurons. Exp. Cell Res. *264*, 266–274.

Augustinack, J.C., Schneider, A., Mandelkow, E.M., and Hyman, B.T. (2002). Specific tau phosphorylation sites correlate with severity of neuronal cytopathology in Alzheimer's disease. Acta Neuropathol. (Berl.) *103*, 26–35.

Bancroft, J.D., and Stevens, A. (1990). Theory and Practice of Histological Techniques, Third Edition (Edinburgh: Churchill Livingstone).

Baumann, K., Mandelkow, E.M., Biernat, J., Piwnica-Worms, H., and Mandelkow, E. (1993). Abnormal Alzheimer-like phosphorylation of tau-protein by cyclin-dependent kinases cdk2 and cdk5. FEBS Lett. *336*, 417–424.

Bian, F., Nath, R., Sobocinski, G., Booher, R.N., Lipinski, W.J., Callahan, M.J., Pack, A., Wang, K.K., and Walker, L.C. (2002). Axonopathy, tau abnormalities, and dyskinesia, but no neurofibrillary tangles in p25-transgenic mice. J. Comp. Neurol. *446*, 257–266.

Biernat, J., Gustke, N., Drewes, G., Mandelkow, E.M., and Mandelkow, E. (1993). Phosphorylation of Ser262 strongly reduces binding of tau to microtubules: distinction between PHF-like immunoreactivity and microtubule binding. Neuron *11*, 153–163.

Billingsley, M.L., and Kincaid, R.L. (1997). Regulated phosphorylation and dephosphorylation of tau protein: effects on microtubule interaction, intracellular trafficking and neurodegeneration. Biochem. J. *323*, 577–591.

Braak, H., Braak. E., Ohm, T., and Bohl, J. (1988). Silver impregnation of Alzheimer's neurofibrillary changes counterstained for basophilic material and lipofuscin pigment. Stain Technol. *63*, 197–200.

Bu, B., Li, J., Davies, P., and Vincent, I. (2002). Deregulation of cdk5, hyperphosphorylation, and cytoskeletal pathology in the Niemann-Pick type C murine model. J. Neurosci. *22*, 6515–6525.

Duff, K., Knight, H., Refolo, L.M., Sanders, S., Yu, X., Picciano, M., Malester, B., Hutton, M., Adamson, J., Goedert, M., et al. (2000). Characterization of pathology in transgenic mice over-expressing human genomic and cDNA tau transgenes. Neurobiol. Dis. *7*, 87–98.

Flaherty, D.B., Soria, J.P., Tomasiewicz, H.G., and Wood, J.G. (2000). Phosphorylation of human tau protein by microtubule-associated kinases: GSK3beta and cdk5 are key participants. J. Neurosci. Res. *62*, 463–472.

Friedhoff, P., von Bergen, M., Mandelkow, E.M., and Mandelkow, E. (2000). Structure of tau protein and assembly into paired helical filaments. Biochim. Biophys. Acta *1502*, 122–132.

Gotz, J., and Nitsch, R.M. (2001). Compartmentalized tau hyperphosphorylation and increased levels of kinases in transgenic mice. Neuroreport *12*, 2007–2016.

Gotz, J., Chen, F., Van Dorpe, J., and Nitsch, R.M. (2001). Formation of neurofibrillary tangles in P301l tau transgenic mice induced by Abeta 42 fibrils. Science *293*, 1491–1495.

Greenberg, S.G., and Davies, P. (1990). A preparation of Alzheimer paired helical filaments that displays distinct tau proteins by polyacrylamide gel electrophoresis. Proc. Natl. Acad. Sci. USA *87*, 5827–5831.

Grundke-Iqbal, I., Iqbal, K., Quinlan, M., Tung, Y.C., Zaidi, M.S., and Wisniewski, H.M. (1986). Microtubule-associated protein tau. A component of Alzheimer paired helical filaments. J. Biol. Chem. *261*, 6084–6089.

Grynspan, F., Griffin, W.R., Cataldo, A., Katayama, S., and Nixon, R.A. (1997). Active site-directed antibodies identify calpain II as an early-appearing and pervasive component of neurofibrillary pathology in Alzheimer's disease. Brain Res. *763*, 145–158.

Hashiguchi, M., Saito, T., Hisanaga, S.I., and Hashiguchi, T. (2002). Truncation of CDK5 activator p35 induces intensive phosphorylation of Ser202/Thr205 of human tau. J. Biol. Chem. *277*, 44525–44530.

Ishiguro, K., Sato, K., Takamatsu, M., Park, J., Uchida, T., and Imahori, K. (1995). Analysis of phosphorylation of tau with antibodies specific for phosphorylation sites. Neurosci. Lett. *202*, 81–84.

Jackson, G.R., Wiedau-Pazos, M., Sang, T.K., Wagle, N., Brown, C.A., Massachi, S., and Geschwind, D.H. (2002). Human wild-type tau interacts with wingless pathway components and produces neurofibrillary pathology in *Drosophila*. Neuron *34*, 509–519.

Lee, K.Y., Clark, A.W., Rosales, J.L., Chapman, K., Fung, T., and Johnston, R.N. (1999). Elevated neuronal Cdc2-like kinase activity in the Alzheimer disease brain. Neurosci. Res. *34*, 21–29.

Lee, M.S., Kwon, Y.T., Li, M., Peng, J., Friedlander, R.M., and Tsai, L.H. (2000). Neurotoxicity induces cleavage of p35 to p25 by calpain. Nature *405*, 360–364.

Lew, J., Huang, Q.Q., Qi, Z., Winkfein, R.J., Aebersold, R., Hunt, T., and Wang, J.H. (1994). A brain-specific activator of cyclin-dependent kinase 5. Nature *371*, 423–426.

Lewis, J., McGowan, E., Rockwood, J., Melrose, H., Nacharaju, P., Van Slegtenhorst, M., Gwinn-Hardy, K., Paul, M.M., Baker, M., Yu, X., et al. (2000). Neurofibrillary tangles, amyotrophy and progressive motor disturbance in mice expressing mutant (P301L) tau protein. Nat. Genet. *25*, 402–405.

Lewis, J., Dickson, D.W., Lin, W.L., Chisholm, L., Corral, A., Jones, G., Yen, S.H., Sahara, N., Skipper, L., Yager, D., et al. (2001). Enhanced neurofibrillary degeneration in transgenic mice expressing mutant tau and APP. Science *293*, 1487–1491.

Liu, F., Iqbal, K., Grundke-Iqbal, I., and Gong, C.X. (2002). Involvement of aberrant glycosylation in phosphorylation of tau by cdk5 and GSK-3beta. FEBS Lett. *530*, 209–214.

Lucas, J.J., Hernandez, F., Gomez-Ramos, P., Moran, M.A., Hen, R., and Avila, J. (2001). Decreased nuclear beta-catenin, tau hyperphosphorylation and neurodegeneration in GSK-3beta conditional transgenic mice. EMBO J. *20*, 27–39.

Lund, E.T., McKenna, R., Evans, D.B., Sharma, S.K., and Mathews, W.R. (2001). Characterization of the in vitro phosphorylation of human tau by tau protein kinase II (cdk5/p20) using mass spectrometry. J. Neurochem. *76*, 1221–1232.

Michel, G., Mercken, M., Murayama, M., Noguchi, K., Ishiguro, K., Imahori, K., and Takashima, A. (1998). Characterization of tau phosphorylation in glycogen synthase kinase-3beta and cyclin depen-

dent kinase-5 activator (p25) transfected cells. Biochim. Biophys. Acta *1380*, 177–182.

Patrick, G.N., Zukerberg, L., Nikolic, M., de la Monte, S., Dikkes, P., and Tsai, L.H. (1999). Conversion of p35 to p25 deregulates Cdk5 activity and promotes neurodegeneration. Nature *402*, 615–622.

Paudel, H.K., Lew, J., Ali, Z., and Wang, J.H. (1993). Brain proline-directed protein kinase phosphorylates tau on sites that are abnormally phosphorylated in tau associated with Alzheimer's paired helical filaments. J. Biol. Chem. *268*, 23512–23518.

Pei, J.J., Tanaka, T., Tung, Y.C., Braak, E., Iqbal, K., and Grundke-Iqbal, I. (1997). Distribution, levels, and activity of glycogen synthase kinase-3 in the Alzheimer disease brain. J. Neuropathol. Exp. Neurol. *56*, 70–78.

Planel, E., Sun, X., and Takashima, A. (2002). Role of GSK-3β in Alzheimer's disease pathology. Drug Dev. Res. *56*, 491–510.

Rank, K.B., Pauley, A.M., Bhattacharya, K., Wang, Z., Evans, D.B., Fleck, T.J., Johnston, J.A., and Sharma, S.K. (2002). Direct interaction of soluble human recombinant tau protein with Abeta 1–42 results in tau aggregation and hyperphosphorylation by tau protein kinase II. FEBS Lett. *514*, 263–268.

Ratner, N., Bloom, G.S., and Brady, S.T. (1998). A role for cyclin-dependent kinase(s) in the modulation of fast anterograde axonal transport: effects defined by olomoucine and the APC tumor suppressor protein. J. Neurosci. *18*, 7717–7726.

Sengupta, A., Wu, Q.L., Grundke-Iqbal, I., Iqbal, K., and Singh, T.J. (1997). Potentiation of GSK-3 catalysed Alzheimer-like phosphorylation of human tau by cdk5. Mol. Cell. Biochem. *167*, 99–105.

Sengupta, A., Kabat, J., Novak, M., Wu, Q., Grundke-Iqbal, I., and Iqbal, K. (1998). Phosphorylation of tau at both Thr 231 and Ser 262 is required for maximal inhibition of its binding to microtubules. Arch. Biochem. Biophys. *357*, 299–309.

Spittaels, K., Van den, H.C., Van Dorpe, J., Geerts, H., Mercken, M., Bruynseels, K., Lasrado, R., Vandezande, K., Laenen, I., Boon, T., et al. (2000). Glycogen synthase kinase-3 beta phosphorylates protein tau and rescues the axonopathy in the central nervous system of human four-repeat tau transgenic mice. J. Biol. Chem. *275*, 41340–41349.

Takashima, A., Noguchi, K., Sato, K., Hoshino, T., and Imahori, K. (1993). Tau protein kinase I is essential for amyloid beta-protein-induced neurotoxicity. Proc. Natl. Acad. Sci. USA *90*, 7789–7793.

Tomidokoro, Y., Ishiguro, K., Harigaya, Y., Matsubara, E., Ikeda, M., Park, J.M., Yasutake, K., Kawarabayashi, T., Okamoto, K., and Shoji, M. (2001). Abeta amyloidosis induces the initial stage of tau accumulation in APP(Sw) mice. Neurosci. Lett. *299*, 169–172.

Town, T., Zolton, J., Shaffner, R., Schnell, B., Crescentini, R., Wu, Y., Zeng, J., DelleDonne, A., Obregon, D., Tan, J., et al. (2002). p35/Cdk5 pathway mediates soluble amyloid-beta peptide-induced tau phosphorylation in vitro. J. Neurosci. Res. *69*, 362–372.

Tseng, H.C., Zhou, Y., Shen, Y., and Tsai, L.H. (2002). A survey of cdk5 activator p35 and p25 levels in Alzheimer's disease brains. FEBS Lett. *523*, 58–62.

Tsuji, T., Shimohama, S., Kinura, J., and Shimizu, K. (1998). m-Calpain (calcium-activated neutral proteinase) in Alzheimer's disease brains. Neurosci. Lett. *248*, 109–112.

Veeranna, Shetty, K.T., Amin, N., Grant, P., Albers, R.W., and Pant, H.C. (1996). Inhibition of neuronal cyclin-dependent kinase-5 by staurosporine and purine analogs is independent of activation by Munc-18. Neurochem. Res. *21*, 629–636.

Veeranna, Amin, N.D., Ahn, N.G., Jaffe, H., Winters, C.A., Grant, P., and Pant, H.C. (1998). Mitogen-activated protein kinases (ERK1,2) phosphorylate Lys-Ser-Pre (KSP) repeats in neurofilament proteins NF-H and NF-M. J. Neurosci. *18*, 4008–4021.

Williamson, R., Scales, T., Clark, B.R., Gibb, G., Reynolds, C.H., Kellie, S., Bird, I.N., Varndell, I.M., Sheppard, P.W., Everall, I., et al. (2002). Rapid tyrosine phosphorylation of neuronal proteins including tau and focal adhesion kinase in response to amyloid-beta peptide exposure: involvement of Src family protein kinases. J. Neurosci. *22*, 10–20.

Yamaguchi, H., Ishiguro, K., Uchida, T., Takashima, A., Lemere, C.A., and Imahori, K. (1996). Preferential labeling of Alzheimer neurofibrillary tangles with antisera for tau protein kinase (TPK) I/glycogen synthase kinase-3 beta and cyclin-dependent kinase *5*, a component of TPK II. Acta Neuropathol. (Berl.) *92*, 232–241.